Proc. Natl. Acad. Sci. USA
Vol. 85, pp. 8732–8736, November 1988
Neurobiology

Magnetic localization of neuronal activity in the human brain

(neuromagnetism/cortical activity/superconductivity quantum interference device)

T. YAMAMOTO*¶, S. J. WILLIAMSON*†, L. KAUFMAN*‡, C. NICHOLSON*, AND R. LLINÁS*§

*Department of Physiology and Biophysics, New York University Medical Center, New York, NY 10016; and Departments of †Physics and ‡Psychology, New York University Faculty of Arts and Sciences, New York, NY 10003

Contributed by R. Llinás, August 10, 1988

ABSTRACT **The performance of a cryogenic system that monitors the extracranial magnetic field simultaneously at 14 positions over the scalp has been evaluated to determine the accuracy with which neuronal activity can be located within the human brain. Initially, measurements were implemented on two model systems, a lucite sphere filled with saline and a model skull. With a magnetic field strength similar to that of a human brain, the measurement and analysis procedures demonstrated a position accuracy better than 3 mm, for a current dipole 3 cm beneath the surface. Subsequently, measurements of the magnetic field pattern appearing 100 ms after the onset of an auditory tone-burst stimulus were obtained in three human subjects. The location of the current dipole representing intracellular ionic current in active neurons of the brain was determined, with 3-mm accuracy, to be within the cortex forming the floor of the Sylvian fissure of the individual subjects, corresponding closely to the Heschl gyrus as determined from magnetic resonance images. With the sensors placed at appropriate positions, the locations of neuronal sources for different tone frequencies could be obtained without moving the recording instrument. Adaptation of activity in human auditory cortex was shown to reveal long-term features with a paradigm that compared response amplitudes for three tones randomly presented.**

Locating neuronal activity within the human brain by measuring the concomitant extracranial magnetic field pattern has been a laborious procedure with single-sensor instruments. Typically, 40 or more positions must be sequentially measured over the scalp, which may take as long as 6 hr to complete. The development of multisensor systems (1–4) made it possible to improve the efficiency of this process, an advance that is of considerable importance for both clinical and research applications. We have installed, at the New York University Medical Center, a commercially available 14-sensor system (Biomagnetic Technologies, San Diego, CA) representing state-of-the-art performance and have evaluated techniques to locate accurately the three-dimensional position of neuronal activity within the human brain (the 14-sensor system consists of two model 607 neuromagnetometers).

The effectiveness of these systems has been evaluated through measurements on two types of carefully designed physical models or "phantoms" (a lucite sphere and a plastic skull), both containing a conducting fluid in which an electrical current dipole was placed at a known position. Measurements were made with field strengths at physiological levels (500 fT); this is an important distinction between this and prior studies (5, 6). To determine the relevance of such localization to human measurements, we investigated the auditory-evoked magnetic field for tone bursts and compared the deduced locations of neural activity with the particular anatomical features of each individual as revealed by magnetic resonance images (MRIs). We then implemented a procedure that permitted source localization without having to move the sensors, a method that greatly speeds the process and allows this technique to be routinely applicable to clinical research and diagnostics for the first time. To illustrate a use of this methodology, we studied an adaptation phenomenon and demonstrated that reduction of signal strength is not a consequence of the cortical shifting to a different location or position but is a modulation of amplitude of a given population of neurons.

We chose to study the auditory modality of human subjects because neuromagnetic measurements have revealed interesting spatial organizations of functions not previously observed in humans—e.g., tonotopic map (7, 8) and amplitopic map (9). There is considerable interest in determining whether these features can be identified with activity in the auditory cortex. Despite numerous electrical (10) and magnetic (11–17) experiments involving this modality, variations in the cortical anatomy across subjects have not yet been shown to affect these measures. It should be noted that localization of equivalent current dipole sources for interictal epileptiform activity based on neuromagnetic measures has agreed with the positions of large lesions seen in computerized tomography (CT) scans (18–20), but even in these cases there was no *a priori* knowledge that the activity should be associated with the particular area of the lesion.

Obtaining the position of a localized source from a field map across the scalp is conceptually simple if neuronal activity is sufficiently well confined to enable it to be modeled as an equivalent current dipole, representing the net orientation and strength of current. The methods for locating such a source have been summarized (21). The procedure is particularly simple when the head may be modeled by a conducting volume of special symmetry, such as a sphere where electrical conductivity depends only on the distance from the center. Since the magnetic field loops around the axis of the dipole, there is one region of the head where the field emerges and another where it enters. The source lies below the center of the pattern, and its depth is determined by the ratio of the distance between the two extrema of the radial field component and the radius of the head. The deeper the source, the greater the distance between field extrema. When the spherical model is applied to a human head the sphere is chosen to characterize the curvature of the inner surface of the skull overlying the approximate position of the dipole. The choice of this criterion was motivated by predictions of numerical modeling that only the conducting medium of the brain need be taken into account, for the currents that diffuse through the skull are too weak to affect appreciably the measured field (22). Moreover, the region of

The publication costs of this article were defrayed in part by page charge payment. This article must therefore be hereby marked "*advertisement*" in accordance with 18 U.S.C. §1734 solely to indicate this fact.

Abbreviations: MRI, magnetic resonance image; PPI, probe position indicator; SQUID, superconducting quantum interference device.

§To whom reprint requests should be addressed.
¶Present address: Department of Otolaryngology, Faculty of Medicine, Kyushu University, Fukuoka, 812, Japan.

the skull directly over the source appears to provide the greatest effect on the external field pattern (23).

METHODS AND RESULTS

Magnetic Sensing System. The neuromagnetic measuring system consists of (Fig. 1*A*) a magnetically shielded room to reduce the effect of ambient field noise and radio frequency signals, two cryogenic dewars holding liquid helium in which the magnetic sensors are suspended, gantries to support the dewars from the ceiling of the shielded room, a probe position indicator (PPI) consisting of a transmitter on each dewar and set of three receivers placed on a band about the subject's head to determine the position and orientation of the sensors with respect to the head, and a bed or chair for the subject. Each dewar contains a set of seven sensors whose detection coils (Fig. 1*B*) are oriented so they point to the approximate center of the subject's head. The bottom of each outer coil is mounted 2 cm from the axis of the center coil. Each detection coil has the geometry of a second-order gradiometer (three coaxial coils connected in series, the center coil having twice as many turns as the bottom and top coils, and wound in the opposite sense) to further reduce the effect of residual magnetic noise within the shielded room. The diameter of the detection coil is 1.5 cm, and the baselength between adjacent coils is 3.7 cm. The detection coil is coupled to a superconducting quantum interference device (SQUID) located higher in the dewar and the SQUID's response to a field is monitored by a set of room temperature electronics whose voltage output is proportional to the net magnetic flux threading the detection coil. The system, therefore, responds to signals within the bandwidth from dc to several kilohertz. A complement of amplifiers and bandpass filters process the signals from the set of 14 SQUIDs before recording on a computer. An additional four SQUIDs and detection coils are included in each dewar to further reduce field noise by adaptive filtering procedures, but they were not needed for the studies reported here.

Head-Based Coordinate System. All measurements were referred to a three-dimensional coordinate system based on the subject's periauricular points and nasion. The axes of this system are defined by touching these positions in turn with a stylus connected to the PPI. The origin of the head-based system is defined as the midpoint between the periauricular points. The x axis is defined as the line from the origin that passes through the nasion. The z axis is defined as the line passing upward from the origin in a direction that is perpendicular to the plane defined by the x axis and the line joining the periauricular points. Finally, the y axis is defined as the line passing out of the left side of the head from the origin, lying perpendicular to the x and z axes. All sensor measurement positions about the head are specified in this head-based system by the PPI.

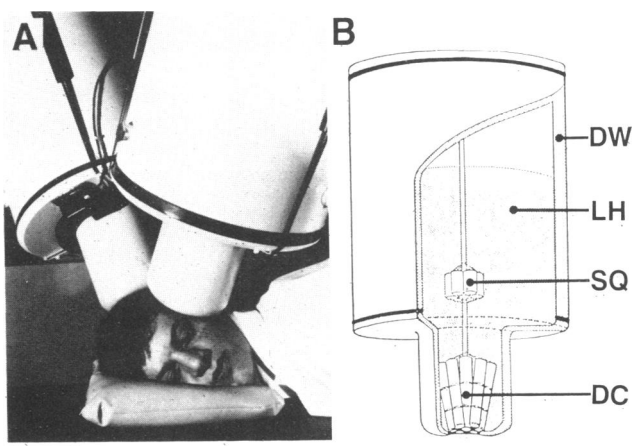

FIG. 1. (*A*) Neuromagnetic system located in a magnetically shielded room. Two dewars are suspended over the subject's head in the positions used to record activity of auditory cortex of the left hemisphere. (*B*) Each dewar (DW) contains liquid helium (LH), seven SQUIDs (SQ), and respective detection coils (DC). Detection coils are wound of superconducting wire and supported by an insulating mount so they all point to a position that is close to the center of the subject's head.

Model Sphere. The first evaluation of this system was carried out through measurements of the field pattern from a current dipole placed within a spherical conductor (Fig. 2*A*). A Lucite sphere with an inner radius of 10.5 cm and a thickness of 2 mm was filled by a saline solution, and a hole through the bottom permitted an insulating rod to be inserted and held at various positions inside. Attached to the rod was a tightly twisted pair of insulated fine wires whose end segments formed the top of a "T" at the end of the rod, with tips exposed to permit current to flow into the solution. This provided a current dipole 5 mm long. The current (58 nA · m) was sufficient to produce a peak field at the sphere's surface of about 500 fT. A Velcro band attached three PPI receivers to the sphere at widely separated noncolinear positions. The PPI stylus was touched to positions marked on the sphere representing the periauricular points and nasion, and these were recorded automatically to establish a head-based coordinate system. The two dewars were oriented at about 30° and 45° from the vertical so their sensors could monitor fields on opposite sides of the dipole. A sinusoidal current (10 Hz) was passed through the current dipole, and the corresponding magnetic field was averaged for 1000 periods. The bandwidth of recording was 1–50 Hz. After each measurement, the sphere was turned about a vertical axis so measurements could be made at another pair of positions. The PPI automatically computed the new positions of each sensor in head-based coordinates.

To obtain a qualitative appreciation of the field pattern, an isofield contour map was produced, with minimal smoothing defining the contours (Fig. 2*B*). The classic field pattern of a current dipole was obtained with a region of outward directed field and another of inward directed field on opposite sides of the dipole. Some irregularity in the contours came from the fact that not all of the sensors are oriented radially for each position. While this affected the smoothness of the contours, it did not affect the accuracy of the program that determines the location, orientation, and moment of the current dipole; since the program takes into account the actual orientation of the sensor with respect to the surface of the sphere.

This procedure was repeated 32 times over a 1-month period to determine the reproducibility of the method. The corresponding deduced positions of the dipole are compared in Fig. 2*C* with the actual position obtained from x-rays of the setup. All of the positions lie within 3 mm of the actual source position.

Model Skull. To confirm the above measurements by using a non-radially symmetric model, a similar procedure evaluated the accuracy of locating a current dipole within a model skull. The model consisted of a plastic skull whose eye sockets and lower edge were sealed to contain a saline solution. A current dipole was inserted upward from the base, to lie approximately 3 cm beneath the skull in the left posterior frontal area. The shape of the outer surface of the skull over a circular area with a radius of approximately 5 cm centered over the dipole was digitized with the PPI stylus. The position was determined by computer for the center of the best-fitting sphere to model the cranium. Magnetic measurement procedures were similar to those for the sphere just described, except that the individual dewars were moved from one place to another to record field values. Approximately 63 sensor positions were recorded in a session. This

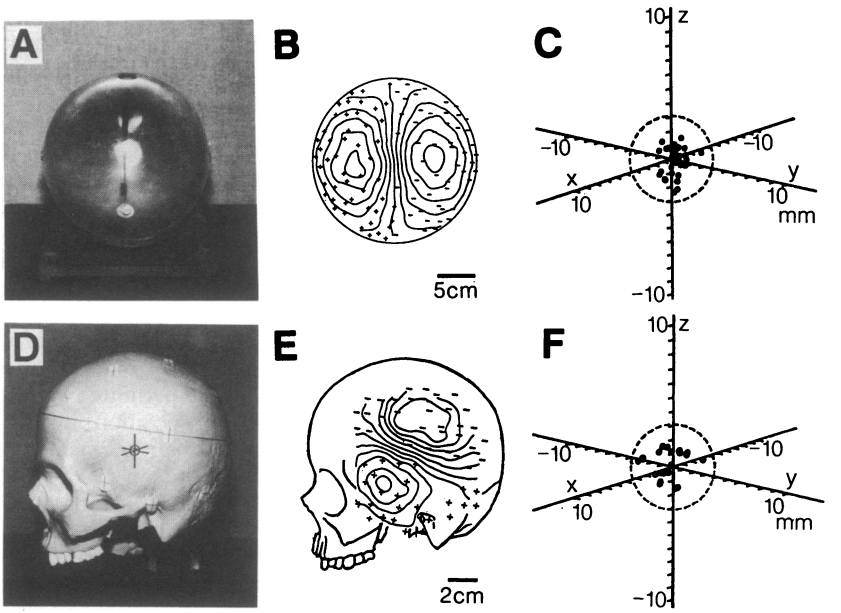

FIG. 2. (*A*) Lucite sphere with current dipole supported by a rod inside it. (*B*) Isofield contours at 100-fT intervals obtained from field values measured at locations denoted by + (field emerging from the surface) and − (field entering the surface). (*C*) Corresponding deduced locations of the current dipole for 32 sets of measurements, with the origin denoting the actual location of the dipole. (*D*) Plastic model skull with an indication of the position above a current dipole held inside. (*E*) Isofield contours at 100-fT intervals projected onto the skull to illustrate the area over which measurements were obtained. (*F*) Corresponding deduced locations of the current dipole for 22 sets of measurements, with the origin denoting the actual location of the dipole.

was repeated 22 times over a period of several days. A representative isofield contour map is shown in Fig. 2*E* in relationship to the skull. The accuracy in determining the location of the dipole was virtually the same (Fig. 2*F*) as for the sphere described earlier. All the deduced locations lie well within 3 mm of the actual location determined by computerized tomography scans.

Auditory Evoked Responses. The third study in this series assessed the accuracy of this procedure in locating an equivalent current dipole source within the human head. Three right-handed volunteers were studied by the same method as for the model skull, except that a circle on the scalp with a radius of about 5 cm with its center approximately 7 cm above the ear canal was digitally characterized for fitting the sphere model. Comparison with MRIs indicated that the thickness of the skull was uniform to within about 20% over this area, so the scalp characterization would yield the same locations for the center of the sphere as the curvature of the inner surface of the skull. Tone burst stimuli with a frequency of about 1 kHz and duration of 400 ms were presented with a random interstimulus interval uniformly distributed within the range of 1.0 to 3.4 s. Stimuli were provided to the right ear through airline style plastic earphones at an intensity of about 70 dB SPL. For each position 100 responses were averaged. The entire recording procedure took 60 min to obtain measurements at 64 sensor positions over the scalp. In addition, MRI recordings were obtained. The coordinates of positions on the MRI slices were indexed to the head-based coordinate system by attaching markers to the skin when the images were recorded.

Fig. 3 shows representative isofield contours for one subject, displaying the two areas of strongest field. The mid-point of the pattern lies above the ear canal, which is expected for a source lying in auditory cortex. The dots in the MRI scans depict the deduced position of the neuronal source with respect to the three principal cross sections of the head, for slices that pass near the computed location. To within our uncertainty of 3 mm, the source lies within the cortical layer forming a portion of the floor of the Sylvian fissure. Fig. 4 *B* and *D* shows isofield contours for two other subjects. Note that here also the midpoints lie approximately over the ear canal. The corresponding positions of the computed sources are shown in the coronal MRI slices, here enlarged in comparison with those in Fig. 3. Again, the sources lie within

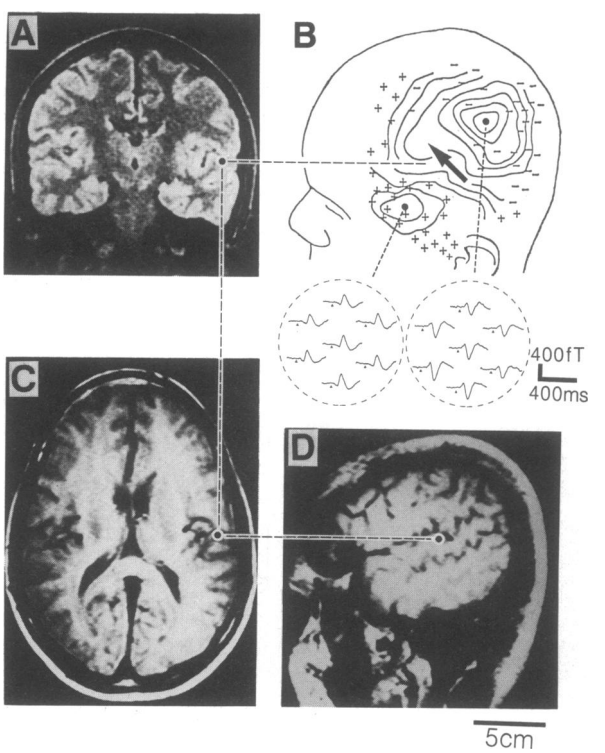

FIG. 3. (*A*, *C*, and *D*) MRI cross sections for subject WH that pass through the deduced location of the source for the 100-ms component of the auditory-evoked response (dots). (*B*) Positions of field measurements and isofield contours for the subject. Also shown are examples of the averaged time-series data obtained by the two seven-sensor dewars near the two-field extrema (100 responses).

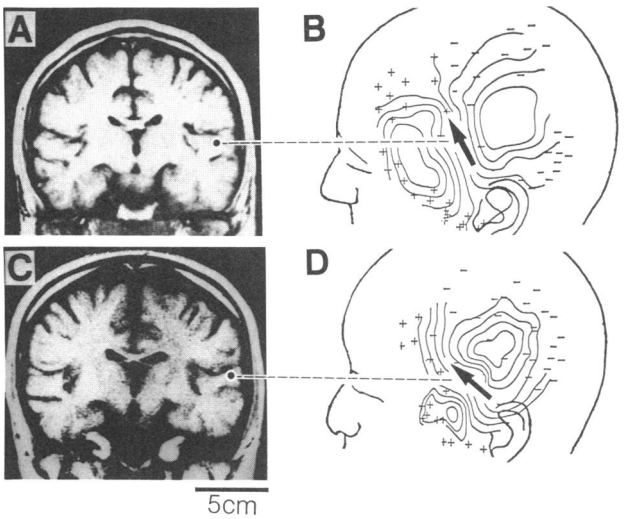

FIG. 4. (*A* and *C*) Portion of the MRI coronal cross sections that pass through the deduced locations of the source for the 100-ms component of the auditory-evoked response (dots), for subjects PF and TY, respectively. (*B* and *D*) Positions of field measurements and isofield contours for the subjects.

the cortex forming the floor of the Sylvian fissure. The agreement between the deduced locations and position of the floor of the Sylvian fissure is consistent with the accuracies previously obtained for measurements with the sphere and skull models. Dipole moments for the subjects ranged from 10 to 30 nA·m.

Fixed Position Measurements. The application of neuromagnetic techniques to clinical diagnoses of neuronal disorders will depend very much on how quickly measurements can be carried out. To assess the ability of the present system to quickly characterize features of the tonotopic representation in human, where tones of higher frequency evoke activity deeper within the head, measurements were obtained with the dewars at fixed locations as close to the field extrema as possible. Tone bursts of 400 ms duration having frequencies of 0.75, 1.00, 1.25, and 1.50 kHz were presented to the right ear in random order. It was possible to fit the 14 recorded average amplitudes of the N100 magnetic component on the left hemisphere by a field pattern produced by a current dipole. The resulting uncertainty in lateral position was 4 mm and the uncertainty in depth was 3 mm. On 11 days the tonotopic sequence was determined over a single octave in frequency for one subject. These results are illustrated in Fig. 5. Excellent agreement is obtained with the tonotopic trends reported earlier (7–9). The precision of the results is

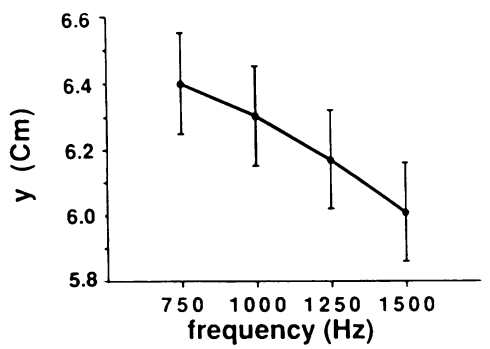

FIG. 5. Coordinates in *y* axis for the source of the 100-ms component of neuronal activity evoked by tone bursts of various frequencies. Bars give the standard error of the mean of the uncertainties (67% confidence levels) for the individual determinations of source locations on separate days.

also consistent with theoretical analyses for such a "fixed position" measurement (24, 25). The measurement time for locating a single source was about 20 min, although the setup time for the subject, including characterizing the scalp surface, was about 20 min.

Adaptation. In carrying out serial measurements on a subject it is essential to minimize adaptation within and across averages. Adaptation effects have long been known in studies of the auditory event-related potential. We employed a paradigm to investigate the phenomenon for both its intrinsic and methodological importance. A total of 700 tones of 1.0, 1.05, or 1.1 kHz were presented in random order, with the interstimulus interval varying randomly between 1.0 and 3.4 s. Separate averages for three subjects were obtained for the N100 amplitude of the first 350 responses and the last 350 responses, when the tone was preceded by the same tone and when preceded by a different tone. Fig. 6 illustrates the difference for the amplitude trends. Cortical neural activity decreases when a tone is preceded by an identical tone but less so when preceded by a different tone, provided there is a sufficient number of prior presentations of the same tone, not necessarily consecutive. Consequently there are short-term as well as long-term features in the response. There was no change in source location or orientation for adapted activity when compared with responses not preceded with the same tone stimulus. Thus each respective area of cortex responding to the particular tones shows this adaptation effect.

DISCUSSION

The preceding results indicate that neuronal activity can be located with high accuracy within the human brain for field strengths at physiological levels, when the geometry of the cranium can be approximated by a spherical model. Accuracy in source location for both the sphere and skull models was consistently better than 3 mm for a current dipole source about 3 cm beneath the surface. Comparable precision, though perhaps not accuracy, may be expected in cases where the spherical model is less representative, as for fronto-temporal areas. In these instances, accuracy can be improved by interpreting the measurements through use of numerical models for the individual's cranium (22, 23).

Comparisons with MRIs of the individual subjects established that the neuronal activity giving rise to the 100-ms components of the auditory-evoked response for a tone burst lies in the floor of the Sylvian fissure, and the orientation of the current dipole is within 10° of being perpendicular to the surface of the cortex. This orientation is consistent with the neuronal currents giving rise to the field being the intracel-

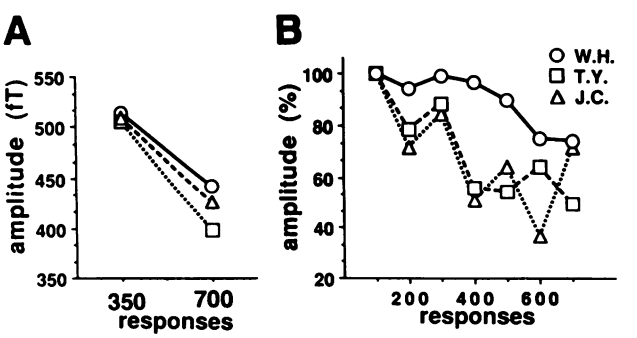

FIG. 6. (*A*) Response amplitude for the 100-ms magnetic component evoked by a tone burst stimulus when a tone is preceded by an identical tone (squares), different tone (circles), or either condition (triangles) for subject WH. Data represent an average of the first and last 350 responses. (*B*) Running average of relative response strengths when a tone is preceded by an identical one, for each of three subjects, averaged over 100 consecutive tone presentations.

lular currents within pyramidal cells, although we cannot rule out other possible sources within the cortex. The position of the source in relation to the ear canal indicates that this portion of cortex is Herschl's gyrus, the location of the auditory cortex. Thus we have established the reliability of the multisensor technique.

Rapid measurements are possible when the approximate locations of the field extrema are known and the two dewars are positioned over them. The possibility of extending this technique to studies of multidimensional functional representations of various modalities is especially attractive. For instance, in the human auditory system, an amplitopic map runs approximately at right angles to the tonotopic axis. Thus, with the "fixed position" paradigm, randomly presented stimuli at various intensities and frequencies can be utilized for a rapid diagnosis of normal or abnormal cortical activity with this truly noninvasive methodology. The prospects with larger arrays of sensors are profound.

While this research has been explicitly concerned with localization of neuronal activity, it is well to keep in mind that the magnitude of such activity is also obtained, as the equivalent current dipole moment. That is, localization provides an objective, quantitative measure of neuronal activity. Thus there is a real prospect that such quantitative measures may have value in diagnosing sensory disorders and disease states.

The adaptation described in this paper is an example where localization demonstrates that reduction in response field amplitude is not due to displacement or rotation of the source, corresponding to a shift of activity from one neuronal population to another, but to reduction in source strength. Adaptation is exhibited by neuronal activity in human auditory cortex with both short-term and long-term features. One significant point to be made is related to randomization of stimuli. For this procedure to be effective in reducing the influence of adaptation on neuromagnetic responses, several different stimuli must be interposed; or perhaps equivalently, more time must be permitted between the presentation of similar stimuli. It is worthwhile to consider whether a dishabituation phenomenon can be demonstrated in this context.

We thank Drs. Wayne Hostetler and Louis Comachia for their invaluable help, Mr. Patrick Fusco and Irene Martin for technical assistance, and Biomagnetic Technologies Inc. for their unfailing technical support during this period of instrumentation development. This work was supported in part by special funds from the New York University Medical Center, the Faculty of Arts and Sciences, Contracts F49620-85-K-0004 and F33615-85-D-0514 from the Air Force Office of Scientific Research, and Grant NS13742 from the National Institutes of Health.

1. Ilmoniemi, R., Hari, R. & Reinikainen, K. (1984) *Electroencephalogr. Clin. Neurophysiol.* **58,** 467–473.
2. Williamson, S. J., Pelizzone, M., Okada, Y., Kaufman, L., Crum, D. B. & Marsden, J. R. (1984) in *ICEC10: Proceedings of the Tenth International Cryogenic Engineering Conference*, eds. Collan, H., Berglund, P. & Krusius, M. (Butterworth, Guildford, UK), pp. 339–348.
3. Romani, G. L., Leoni, R. & Salustri, C. (1985) in *SQUID '85: Superconducting Quantrum Interference Devices*, eds. Hahlbohm, H. D. & Lübbig, H. (de Gruyter, Berlin), pp. 919–932.
4. Knuutila, J., Ahlfors, S., Ahonen, A., Hällström, J., Kajola, M., Lounasmaa, O. V. & Vilkman, V. (1987) *Rev. Sci. Instrum.* **58,** 2145–2156.
5. Barth, D. S., Sutherling, W., Broffman, J. & Beatty, J. (1986) *Electroencephalogr. Clin. Neurophysiol.* **63,** 260–273.
6. Hansen, J. S., Ko, H. W., Fisher, R. S. & Litt, B. (1988) *Phys. Med. Biol.* **33,** 105–111.
7. Romani, G. L., Williamson, S. J. & Kaufman, L. (1982) *Science* **216,** 1339–1341.
8. Romani, G. L., Williamson, S. J., Kaufman, L. & Brenner, D. (1982) *Exp. Brain Res.* **47,** 381–393.
9. Pantew, C., Hoke, M., Lütkenhöner, B. & Lehnertz, K. (1988) in *Biomagnetism '87: Proceedings of the 6th International Conference*, eds. Atsumi, K., Katila, T., Williamson, S. J. & Ueno, S. (Tokyo Denki Univ. Press, Tokyo), pp. 146-149.
10. Vaughan, H. G., Jr., & Ritter, W. (1970) *Electroencephalogr. Clin. Neurophysiol.* **28,** 360–367.
11. Farrell, D. E., Tripp, J. H., Norgren, R. & Teyler, T. J. (1980) *Electroencephalogr. Clin. Neurophysiol.* **49,** 31–37.
12. Elberling, C., Bak, C., Kofoed, B., Lebech, J. & Saermark, K. (1980) *Scand. Audiol.* **9,** 185–190.
13. Hari, R., Aittoniemi, K., Järvinen, M. L., Katila, T. & Varpula, T. (1980) *Exp. Brain Res.* **40,** 237–240.
14. Tuomisto, T., Hari, R., Katila, T., Poutanen, T. & Varpula, T. (1983) *Il Nuovo Cimento* **2D,** 471–483.
15. Sams, M., Hämäläinen, M. S., Antervo, A., Kaukoranta, E., Reinikainen, K. & Hari, R. (1985) *Electroencephalogr. Clin. Neurophysiol.* **61,** 254–266.
16. Pelizzone, M., Williamson, S. J. & Kaufman, L. (1985) in *Biomagnetism: Applications and Theory*, eds. Weinberg, H., Stroink, G. & Katila, T. (Pergamon, New York), pp. 326–330.
17. Arthur, D. L., Flynn, E. R. & Williamson, S. J. (1987) *Electroencephalogr. Clin. Neurophysiol. Supplement* **40,** 429–439.
18. Barth, D. S., Sutherling, W., Engel, J. E., Jr., & Beatty, J. (1984) *Science* **223,** 293–296.
19. Sutherling, W., Crandall, P. H., Cahan, L. D. & Barth, D. S. (1988) *Neurology* **38,** 778–786.
20. Ricci, G. B., Romani, G. L., Salustri, C., Pizzella, V., Torrioli, G., Buonomo, S., Peresson, M. & Modena, I. (1987) *Electroencephalogr. Clin. Neurophysiol.* **66,** 358–368.
21. Williamson, S. J. & Kaufman, L. (1987) in *Handbook of Electroencephalography and Clinical Neurophysiology*, eds. Gevins, A. & Rémond, A. (Elsevier, Amsterdam), Vol. 1 Revised, pp. 405–448.
22. Hämäläinen, M. S. & Sarvas, J. (1988) in *Biomagnetism–88*, eds. Atsumi, K., Kotani, M., Ueno, S., Katila, T. & Williamson, S. J. (Denki Univ. Press, Tokyo), pp. 98–101.
23. Hari, R. & Ilmoniemi, R. J. (1986) *CRC Crit. Rev. Biomed. Eng.* **14,** 93–126.
24. Meijs, J. W. H., Bosch, F. G. C., Peters, M. J. & Lopes da Silva, F. H. (1987) *Electroencephalogr. Clin. Neurophysiol.* **66,** 286–298.
25. Costa Ribeiro, P., Williamson, S. J. & Kaufman, L. (1988) *IEEE Trans. Biomed. Eng.* **35,** 551–560.